

Tracking and Elucidating *Alphavirus*-Host Protein Interactions*[§]

Received for publication, April 26, 2006, and in revised form, July 10, 2006. Published, JBC Papers in Press, August 8, 2006, DOI 10.1074/jbc.M603980200

Ileana M. Cristea[‡], John-William N. Carroll[§], Michael P. Rout[¶], Charles M. Rice[§], Brian T. Chait^{†1}, and Margaret R. MacDonald^{§2}

From the Laboratories of [‡]Mass Spectrometry and Gaseous Ion Chemistry, [§]Virology and Infectious Disease, and [¶]Cellular and Structural Biology, The Rockefeller University, New York, New York 10021

Viral infections cause profound alterations in host cells. Here, we explore the interactions between proteins of the *Alphavirus* Sindbis and host factors during the course of mammalian cell infection. Using a mutant virus expressing the viral nsP3 protein tagged with green fluorescent protein (GFP) we directly observed nsP3 localization and isolated nsP3-interacting proteins at various times after infection. These results revealed that host factor recruitment to nsP3-containing complexes was time dependent, with a specific early and persistent recruitment of G3BP and a later recruitment of 14-3-3 proteins. Expression of GFP-tagged G3BP allowed reciprocal isolation of nsP3 in Sindbis infected cells, as well as the identification of novel G3BP-interacting proteins in both uninfected and infected cells. Noteworthy interactions include nuclear pore complex components whose interactions with G3BP were reduced upon Sindbis infection. This suggests that G3BP is a nuclear transport factor, as hypothesized previously, and that viral infection may alter RNA transport. Immunoelectron microscopy showed that a portion of Sindbis nsP3 is localized at the nuclear envelope, suggesting a possible site of G3BP recruitment to nsP3-containing complexes. Our results demonstrate the utility of using a standard GFP tag to both track viral protein localization and elucidate specific viral-host interactions over time in infected mammalian cells.

The wide range of diseases caused by viruses is a reflection of their diverse interactions with host organisms and manipulation of cellular processes. Discerning the correlation between the localization and interactions of viral proteins in host systems as a function of time can greatly facilitate our understanding of dynamic viral infections, ultimately leading to both improved therapeutics and insight into cellular processes.

* This work was supported by National Institutes of Health Grants AI063233 (to M. R. M.), AI24134 (to C. M. R.), RR00862 (to B. T. C.), RR022220 (to M. P. R. and B. T. C.), and GM062427 (to M. P. R.); by The Rockefeller University Women and Science Fellowship CEN5300379 (to I. M. C.); and by the Greenberg Medical Research Institute. The costs of publication of this article were defrayed in part by the payment of page charges. This article must therefore be hereby marked "advertisement" in accordance with 18 U.S.C. Section 1734 solely to indicate this fact.

[§] The on-line version of this article (available at <http://www.jbc.org>) contains supplemental Figs. S11–S14 and Tables S1 and S2.

¹ To whom correspondence may be addressed: The Rockefeller University, 1230 York Ave., New York, NY 10021. Tel.: 212-327-8849; Fax: 212-327-7547; E-mail: chait@rockefeller.edu.

² To whom correspondence may be addressed: The Rockefeller University, 1230 York Ave., New York, NY 10021. Tel.: 212-327-7078; Fax: 212-327-7048; E-mail: macdonm@rockefeller.edu.

We recently developed a method that uses GFP for the efficient visualization and isolation of protein complexes in living systems (1). Here, we apply this method to study viral protein interactions during the progression of an infection. We selected Sindbis virus for study because it is a genetically amenable member of the *Alphavirus* genus in the *Togaviridae* family, a positive strand RNA virus family known to cause significant diseases (reviewed in Ref. 2). After infection of susceptible cells with Sindbis, the RNA genome is released into the cytoplasm and translated to generate viral proteins necessary for replication. Sequences encoding proteins involved in RNA replication, the nonstructural proteins (nsPs),³ are located in the 5' two-thirds of the viral genome, while the virion structural proteins are encoded by the 3' end of the genome (reviewed in Refs. 3 and 4). Translation of the genomic RNA generates a polyprotein containing nsP1, nsP2, and nsP3, while readthrough of an opal termination codon results in production of nsP1-nsP2-nsP3-nsP4. These polyproteins are then processed by a protease residing in nsP2 to generate the individual nsPs. The nsPs carry out important viral functions, including production of a full-length minus strand RNA, new genomic positive strand RNA, and a subgenomic RNA, which encodes the viral structural proteins. Activities important for these processes have been mapped to specific nsPs (reviewed in Ref. 5); nsP1 is important for capping the RNAs and interacts with membranes, nsP2 contains the aforementioned proteolytic activity, exhibits nucleosidetriphosphatase and helicase activities, and is involved in regulation of RNA synthesis. nsP4 is the viral RNA-dependent RNA polymerase. While known to be essential for viral replication, the functions of nsP3 are not yet understood. Although nsP3 is involved in replication of the viral RNA, the fact that nsP3 is produced in larger amounts than nsP4 suggests that nsP3 may interact with multiple host and viral targets to mediate other activities beneficial to the virus. The sequence of nsP3 is highly conserved among alphaviruses with the exception of the carboxyl-terminal domain that varies in length and sequence. Previous studies showed that deletions

³ The abbreviations used are: nsP, nonstructural protein; GFP, green fluorescent protein; mRFP, monomeric red fluorescent protein; G3BP, Ras-GTPase-activating protein SH3-domain-binding protein; m.o.i., multiplicity of infection; 14-3-3, tyrosine 3-monooxygenase/tryptophan 5-monooxygenase activation protein; hnRNP, heterogeneous nuclear ribonucleoproteins; NTF, nuclear transport factor; TIA, T-cell intracellular antigen; MS, mass spectrometry; MS/MS, tandem MS; EM, electron microscopy; PBS, phosphate-buffered saline; RRM, RNA recognition motif; MALDI, matrix-assisted laser desorption ionization; TTP, tristetraprolin.

Dynamics of Alphavirus nsP3 Interactions

and insertions in the variable nsP3 carboxyl-terminal domain are tolerated (6–8).

Here, we used a mutated Sindbis virus, containing a GFP tag inserted in frame within the carboxyl-terminal domain of nsP3 (6), to visualize nsP3 and concomitantly identify its host and viral interacting partners. To ascertain the specificity of the observed interactions, we utilized a control virus expressing free GFP, reciprocal immunoisolations of host proteins and colocalization studies. We monitored the dynamics of viral-host interactions during the course of Sindbis infection so as to gain insight into nsP3 function in viral replication and the alteration of cellular processes. These methods are broadly applicable to the study of diverse viral systems.

EXPERIMENTAL PROCEDURES

Cell Lines—Rat2 fibroblast cells (ATCC CRL-1764) and human HEK293 cells were grown at 37 °C in a humidified chamber containing 5% CO₂ in Dulbecco's modified Eagle's medium supplemented with 10% fetal bovine serum (Invitrogen). Cell lines stably expressing GFP-tagged G3BP and domains A–D were generated by transfection of HEK293 cells with expression constructs using FuGENE 6 (Roche Diagnostics) according to the manufacturer's directions, followed by selection in the presence of medium containing 1 mg/ml G418 (Invitrogen).

Plasmids and Viruses—Sindbis, Ross River, and Yellow fever virus stocks were prepared as described previously (8). Wild-type Sindbis utilized in these studies was generated from plasmid pToto1101 (9). Virus expressing enhanced GFP as an in-frame fusion within nsP3 was described previously (6) and is here designated nsP3-GFP Sindbis. Sequences encoding mRFP-1 (10) were cloned in the SpeI site generating pToto1101/mRFP-1; the resulting virus is designated nsP3-mRFP-1 Sindbis. pTE/5'2J-GFP (described in Ref. 11) contains sequences encoding enhanced GFP downstream of an engineered extra subgenomic promoter. The generated virus expresses free GFP from a 5' subgenomic RNA and the viral structural proteins from a 3' subgenomic RNA and is here designated Control GFP Sindbis. Plasmids expressing GFP-tagged G3BP1 or domains A–D of G3BP1 were described previously (12).

Antibodies—Antibodies directed against the following human proteins were used at the indicated dilutions for immunofluorescence analyses: G3BP1, mouse monoclonal, 1:1000 (611126, BD Transduction Laboratories); 14-3-3 ϵ , rabbit polyclonal, 1:50 (sc-1020, Santa Cruz Biotechnology); heterogeneous nuclear ribonucleoprotein (hnRNP) A2/B1, goat polyclonal, 1:50 (sc-10035, Santa Cruz Biotechnology); hnRNP A3, goat polyclonal, 1:100 (sc-16542, Santa Cruz Biotechnology); hnRNP G, goat polyclonal, 1:50 (sc-14581, Santa Cruz Biotechnology). Anti-Sindbis capsid rabbit polyclonal (13), which cross-reacts with the Ross River capsid protein, was diluted 1:250 to 1:1000, while anti-Yellow fever NS4 (14) polyclonal serum was diluted 1:500. Rhodamine Red-X-conjugated AffiniPure donkey anti-mouse, donkey anti-goat and donkey anti-rabbit IgG antibodies (Jackson ImmunoResearch Laboratories) were diluted 1:200. Alexa Fluor 594 goat anti-mouse IgG and Alexa Fluor 488 goat anti-rabbit antibodies (Molecular Probes) were diluted 1:1000. Cus-

tom high titer anti-GFP polyclonal antibodies were prepared at Covance (Denver, PA) using an in-house prepared GFP to inject female Elite rabbits as described previously (1). The anti-GFP polyclonal antibodies were then affinity purified on GFP-conjugated CNBr-activated Sepharose 4B resin (GE Healthcare) following standard affinity purification procedures (15). Western analyses utilized the anti-GFP antibodies (1:3000–1:6000) as well as anti-14-3-3 ϵ mouse monoclonal (Invitrogen 39-7600, 1:200) and anti- β -actin mouse monoclonal (Sigma A5441, 1:5,000) antibodies. Polyclonal rabbit antibodies, generated against bacterially expressed amino acids 355–501 of Sindbis nsP3⁴ were utilized at 1:1000 dilution. Horseradish peroxidase-conjugated secondary antibodies (Pierce) were diluted 1:10,000–1:20,000.

Cell Disruption, Extraction, and Immunoaffinity Purification—Cultured cells, grown to ~70% confluence, were harvested in phosphate-buffered saline (PBS) by scraping with a rubber policeman. After PBS washing and centrifugation, the cell pellet was weighed and resuspended (0.1 ml/g) in 20 mM HEPES, pH 7.5, 1.2% (w/v) polyvinylproline, and protease inhibitors. The cells, frozen as small pellets by dropping into liquid nitrogen, were loaded in round-bottom Eppendorf tubes. One 2-mm stainless steel grinding ball was placed in the middle of the sample to prevent cracking of the tube. Cells were lysed cryogenically in 6 steps of 3 min at 30 Hz using the Retsch MM 301 Mixer Mill (Retsch, Newtown, PA). Cell disruption efficiency was confirmed by light microscopy. The cell powder was homogenized in lysis buffer as described (1). We tested several buffers for efficient protein extraction and maintenance of viral-host protein interactions. Based on a previous work isolating biochemically active Sindbis replication complexes (16), our optimized lysis buffer was 20 mM K-HEPES, pH 7.4, 110 mM KOAc, 2 mM MgCl₂, 0.1% Tween 20, 1% Triton, 0.5% deoxycholate, 0.5 M NaCl, 25 units/ml DNase, 1/100 (v/v) protease inhibitor mixture (20 mg/ml phenylmethylsulfonyl fluoride + 0.4 mg/ml pepstatin A), and 1/200 (v/v) protease inhibitor mixture (Sigma). Immunoaffinity purifications were performed as described (1) using 1-h incubations with M-270 Epoxy Dynabeads (Dyna, Lake Success, NY) coupled to in-house prepared anti-GFP antibodies.

Mass Spectrometry—Isolated proteins were resolved by one-dimensional SDS-PAGE. Each entire gel lane was cut into 1–2-mm pieces and proteins digested with trypsin and analyzed by mass spectrometry (17) using MALDI QqToF MS and MALDI IT MS/MS as described (1).

Immunofluorescent Microscopy—Cells were seeded onto collagen-coated coverslips or 4-well slides and were infected or mock infected prior to fixation with 3.7% formaldehyde in PBS. Nuclei were stained with 0.8 μ M bisbenzimidazole (Sigma, Hoechst No. 33258) in PBS containing 0.2% saponin. For indirect immunofluorescence, samples were blocked in PBS containing 0.2% saponin and 10% goat serum. Sequential incubations with primary and secondary antibodies were performed in PBS with 0.05% saponin/10% goat serum, and nuclei were stained as above. The samples were mounted in PBS with 90% glycerol

⁴ M. V. Soukhodolets and C. M. Rice, unpublished data.

and visualized on a Nikon Eclipse TE300 inverted microscope equipped with a TE-FM epifluorescence attachment, mercury lamp power supply, and a Spot RT camera (model 2.2.1, Diagnostic Instruments). Images were acquired with a 100 \times oil immersion objective using the Spot software.

Confocal Microscopy—Cells were seeded onto collagen coated coverslips and after infection were fixed as described above or with 1% paraformaldehyde in PBS. Nuclei were stained with 4 μ M TO-PRO-3 (Molecular Probes) in PBS with 0.05% saponin and were mounted as described above. For indirect immunofluorescence, samples were treated as described above, but 2% bovine serum albumin was utilized in place of the goat serum, and nuclei were stained by incubation with 5 μ M TO-PRO-3 in PBS. Cells were mounted as described above and visualized in the Rockefeller University Bio-Imaging Resource Center utilizing a Zeiss LSM 510 upright Axioplan confocal microscope equipped with a HeNe laser (633 line), and a Krypton/Argon laser (488 and 568 lines) or an Argon laser (488 line) and a HeNe laser (543 line). Images were acquired with either a 63x/1.2 NA C-Apochromat or a 40x/1.2 NA C-Apochromat water immersion objective using the LSM software.

Electron Microscopy (EM)—EM analyses were conducted in The Rockefeller University Bio-Imaging Resource Center using a JEOL 100 cx electron microscope operated at 80 kV. Rat2 cells were mock infected or infected for 12 h with nsP3-GFP Sindbis (m.o.i. \sim 10–15), fixed for morphological analysis with 2.5% glutaraldehyde in 0.1 M cacodylate, pH 7.4, and post-fixed in 1% osmium tetroxide. The samples were processed by routine transmission EM techniques and were embedded in EMBED 812 (Electron Microscopy Sciences, Hatfield, PA). For immuno-EM, cells were fixed in 2% paraformaldehyde, 1% glutaraldehyde in 0.1 M cacodylate, pH 7.4, and ultrathin cryosections were prepared and labeled as described (18, 19) with anti-GFP antiserum (1:2000) and secondary antibodies conjugated to 10-nm gold particles (Amersham Biosciences). Scans of the negatives were used to generate the images shown using Adobe Photoshop software.

RESULTS AND DISCUSSION

Strategy for Visualizing Viral Proteins in Host Cells and Isolating Their Interacting Partners—We used a four-step strategy to study viral protein interactions in host systems. The method is illustrated in Fig. 1 for the study of Sindbis nsP3. To follow the localization and interactions specific to nsP3 we utilized nsP3-GFP Sindbis, a virus expressing GFP as a fusion with nsP3 (6). The viral polyprotein of this mutant virus is properly post-translationally processed, and the virus replicates to equivalent titers as wild-type virus, with only a slight delay in replication kinetics (6). As a control for nonspecific protein interactions in Sindbis-infected cells we utilized Control GFP Sindbis (11), a virus expressing free GFP. Upon infection of Rat2 cells, the free GFP was diffusely localized in the nucleus and cytoplasm, whereas nsP3-GFP was localized to distinct cytoplasmic foci, as observed previously for nsP3 (6, 20, 21). In parallel with visualization, the cells were rapidly frozen and cryogenically lysed to help preserve protein complexes close to their original cellular state. The cell lysates were used for immunoaffinity purifications on magnetic beads coated with polyclonal anti-GFP anti-

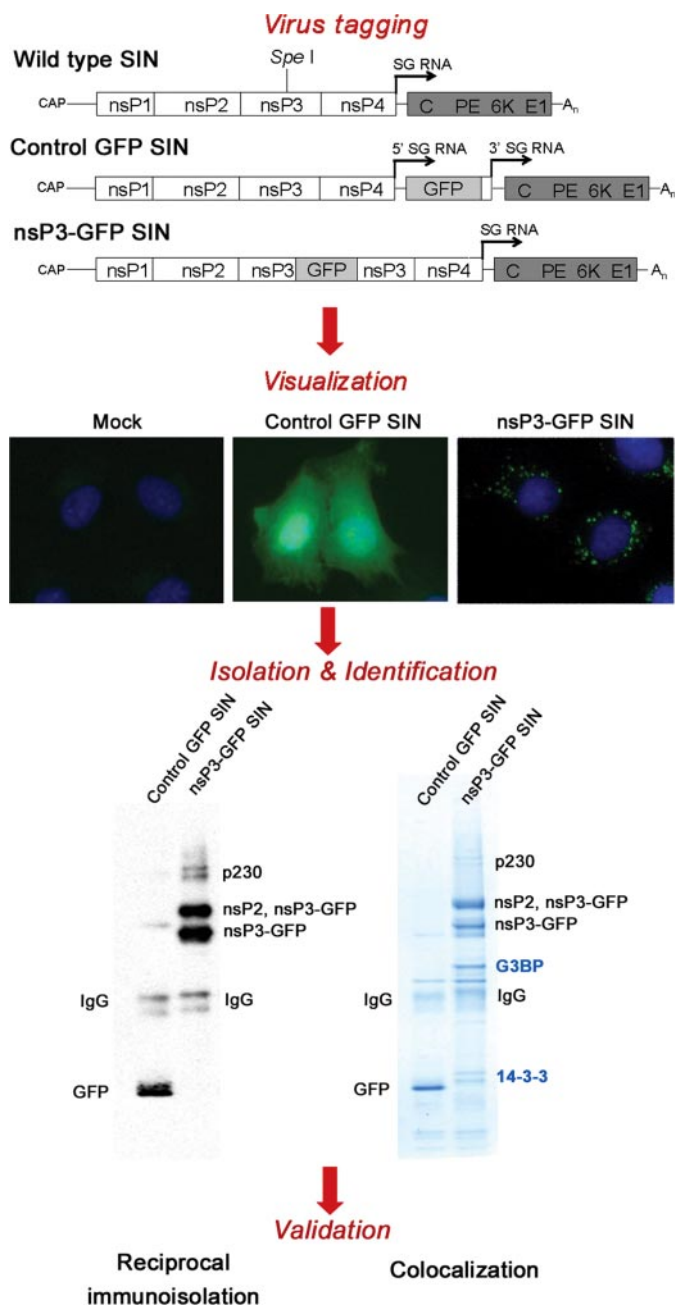


FIGURE 1. Strategy for the visualization and isolation of viral proteins via a GFP tag. *Top*, schematic representations of Sindbis (SIN) genomes; nsPs and structural genes (C, PE, 6K, E1) are indicated. *Arrows* show transcription sites for the subgenomic RNAs. *Center*, visualization of GFP expressed by the Sindbis mutants. Rat2 cells were mock infected or infected (m.o.i. \sim 10) with the indicated virus, fixed 4.5 h post-infection, and analyzed by fluorescence microscopy. The merged *blue* (nuclei) and *green* (GFP) images are shown. *Bottom*, immunoaffinity purifications via the GFP tag from cells infected for 12 h with the indicated viruses. The isolated proteins were resolved by SDS-PAGE and identified by MS (*right*). Western blot using anti-GFP antibodies is shown (*left*). Validation of the observed interactions was carried out using reciprocal immunoprecipitations and co-localization experiments. p230, nsP1–nsP2–nsP3. Bands due to IgG heavy chain or secondary reactivity to IgG heavy chain are indicated. The faint bands observed in the upper region of the Control GFP Sindbis Western blot are also likely due to secondary antibody binding to multimers of IgG. MS and MS/MS analyses did not reveal any viral proteins in the control GFP Sindbis lane.

bodies, and the purified proteins were identified by mass spectrometry (1). Our protocols have been optimized to obtain an efficient recovery of nsP3-GFP, as shown by the major Coomas-

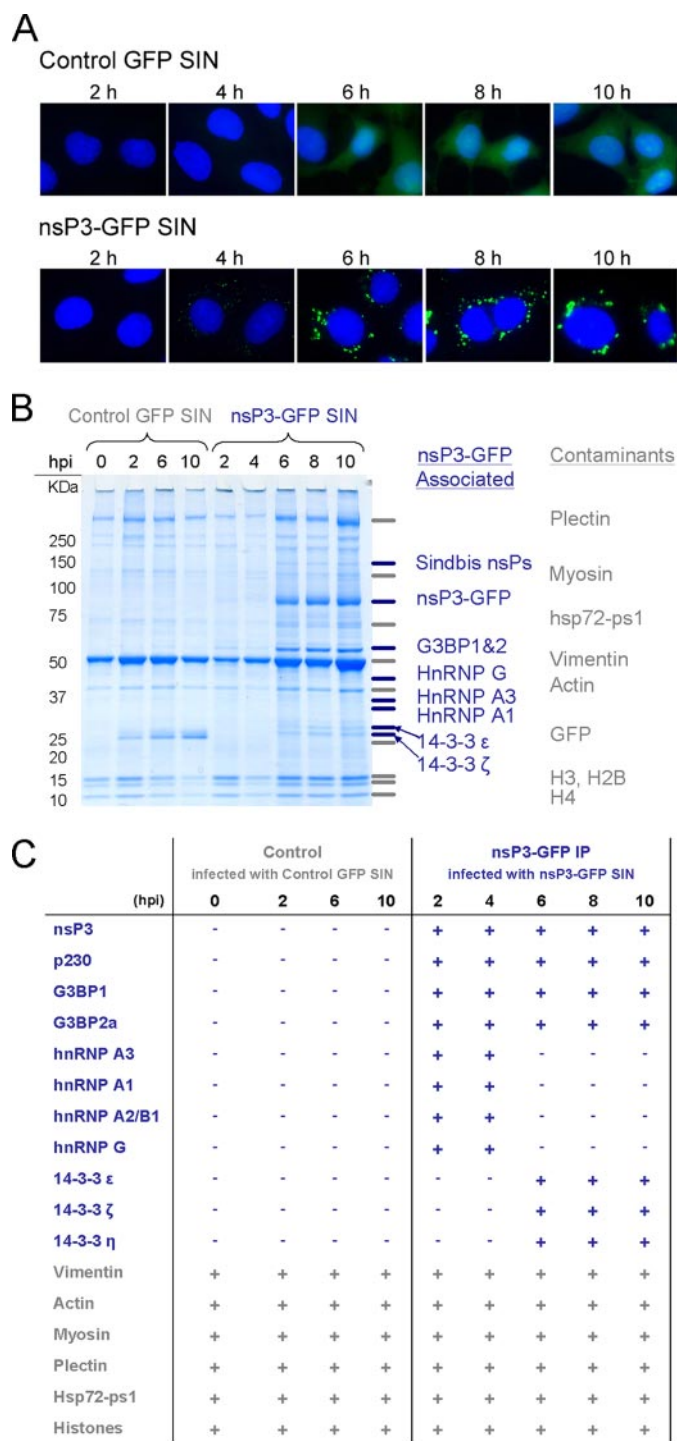


FIGURE 2. Profiling viral-host protein interactions during the course of infection. A, GFP visualization by immunofluorescent microscopy at various times after infection of Rat2 cells with Control GFP Sindbis and nsP3-GFP Sindbis. B, immunoaffinity purifications were performed from control and nsP3-GFP samples at different stages of infection. Immunoprecipitated proteins were separated by SDS-PAGE. A selection of specific (blue) and nonspecific (gray) associated proteins are labeled. C, table indicating the presence (+) or absence (-) of the selected proteins at each time point of infection.

sie Blue-stained band on our SDS-PAGE of the isolated material (Figs. 1 and 2). For validation of identified host factors, we used several methods. First, as mentioned above, we used a control virus, expressing free GFP, to address cellular proteome changes solely due to viral infection and discriminate the

potentially specific interactions. Second, we performed co-localization studies for these potential interacting partners. Third, we immunoprecipitated the host factor to test for the presence of a specific nsP3 interaction.

Determination of Viral-Host Interactions as a Function of Infection Time—To follow the dynamics of viral-host protein interactions during the course of infection, we visualized (Fig. 2A) and isolated (Fig. 2B) free GFP and GFP-tagged nsP3 after 2, 4, 6, 8, and 10 h of infection with Control GFP Sindbis or nsP3-GFP Sindbis, respectively. Comparisons between the control and nsP3 isolations at these stages of infection in replicate experiments discriminated interactions specific to nsP3 from nonspecific interactions (Fig. 2C). Most proteins observed in our control immunoprecipitations were highly abundant cytoskeletal proteins we often encounter as nonspecific binding proteins in isolations from mammalian lysates. These same nonspecific binding proteins were observed in the nsP3-GFP isolations, albeit with higher abundance. Although we cannot exclude specific interactions with these cytoskeletal proteins, their higher abundance is likely the result of additional nonspecific binding to nsP3-GFP or to its specific binding partners, a phenomenon that we have documented extensively in the immunoprecipitation of proteins (1, 22).

Certain proteins were consistently associated with nsP3 throughout the course of infection. For example, G3BP1 and G3BP2 (Ras-GTPase-activating protein SH3-domain-binding protein) were present abundantly at all time points of infection (MS and MS/MS data shown in supplemental Figs. S11 and S12). Conversely, the recruitment of other host proteins to nsP3-containing complexes was time-regulated; examples include the hnRNPs A1, A3, A2/B1, and G, detected primarily at the early times of infection, and 14-3-3 ε, ζ, and η (tyrosine 3-monooxygenase/tryptophan 5-monooxygenase activation proteins ε, ζ, and η), found specifically at the late times of infection. The nsP3 interaction with G3BP and 14-3-3 was also confirmed using human HEK293 fibroblast cells infected for 10 h (data not shown). Supplemental Table S1 provides a complete list of the proteins identified at each time point shown in Fig. 2. A recent publication studied nsP3 interactions at one time point of infection (8 h) using BHK-21 hamster cells (21). Comparing these reported interacting proteins with our data, we noted that seven proteins, including vimentin and myosin, were present in our control samples that test for nonspecific interactions, raising questions as to the specificity of the reported interactions. In our study, of the total 59 identified proteins, 35 were specific to the nsP3 isolations. Ten of these specific proteins were also reported in the recent publication, including G3BP1, 14-3-3 ε and ζ, and several hnRNPs.

In agreement with our immunoaffinity purification results, we observed temporally regulated co-localizations of G3BP1 and 14-3-3 proteins with nsP3 (Fig. 3). G3BP1 co-localized with nsP3-GFP at both early and late times after infection (Fig. 3A). G3BP1, which is virtually undetectable in uninfected Rat2 cells (Fig. 6), becomes readily apparent in infected cells, likely due to subcellular redistribution. We also noted this redistribution in infected human, hamster, and murine cells (data not shown). We observed similar changes in G3BP1 staining in Rat2 cells infected with wild-type Sindbis (Fig. 6), demonstrating that the

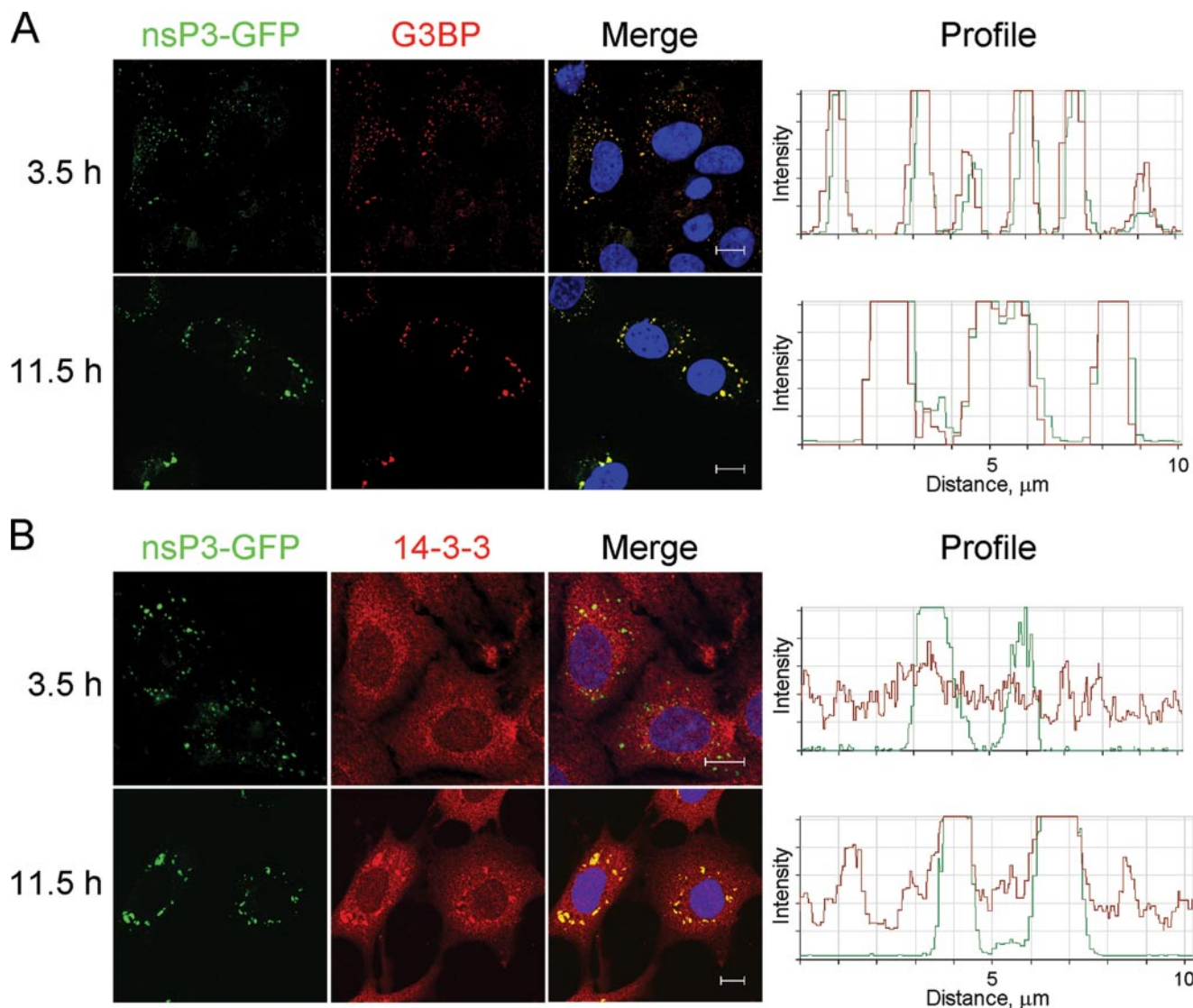


FIGURE 3. G3BP1 and 14-3-3 co-localize with nsP3-GFP. Rat2 cells were infected with nsP3-GFP Sindbis (m.o.i. ~ 70) for the indicated times and analyzed by confocal microscopy. Samples were incubated with antibodies to G3BP (A) or 14-3-3 ϵ (B) and Rhodamine Red-X-conjugated secondary antibodies. Green (left), red (middle), and merged (right) images are shown. Nuclei (blue) are shown in the merged images. Bars, 10 μm . Representative fluorescence intensity profiles are shown to the right.

redistribution was not an artifact of the GFP tag. In agreement with our immunoaffinity purification results, 14-3-3 co-localization with nsP3-GFP was observed only at late times of infection (Fig. 3B). Although foci of 14-3-3 were observed at late times following infection with Control GFP Sindbis, 14-3-3 did not co-localize with the free GFP expressed from this control virus (supplemental Fig. S13). This confirmed that nsP3, and not the GFP tag, was responsible for the 14-3-3 co-localization seen after infection with nsP3-GFP Sindbis. We also observed co-localization of nsP3-GFP with hnRNPs A2/B1, and A3, and partial co-localization with hnRNP G (data not shown).

The apparent association of 14-3-3 with nsP3 only at late stages of infection raised questions to whether this is a truly time-dependent association or rather the result of altered concentrations of these interacting molecules. We therefore assessed the levels of 14-3-3 in infected cells at various times and found that viral infection did not alter 14-3-3 levels (Fig. 4). As expected (see Fig. 2), our results showed an increase in the

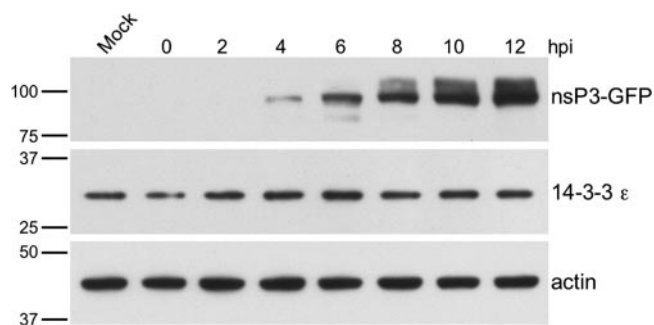


FIGURE 4. Expression of nsP3, 14-3-3, and actin as a function of infection time. Rat2 cells were infected with nsP3-GFP Sindbis (m.o.i. ~ 10) and harvested at the indicated times after infection. Equal protein loading of whole cell lysates were analyzed by Western blot for the indicated proteins.

levels of nsP3 with infection time (Fig. 4). The increased levels of nsP3 at the later time points could influence the nsP3–14-3-3 interaction or its detection. One possibility is that 14-3-3 also

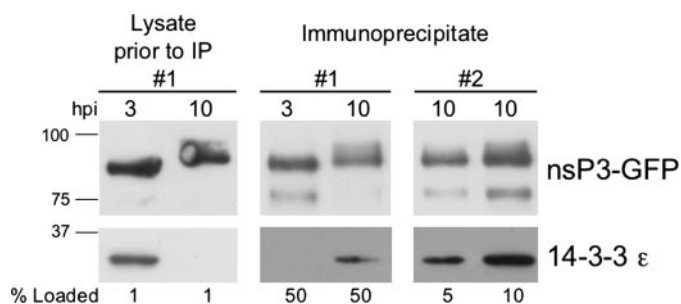


FIGURE 5. The 14-3-3-nsP3 association is infection-time dependent. Rat2 cells were infected with nsP3-GFP Sindbis (m.o.i. ~10) and harvested at 3 and 10 h post-infection. For 3 h post-infection, seven 15-cm dishes were utilized (#1). For 10 h post-infection, two experiments were performed utilizing either one 15-cm dish (#1) or seven dishes (#2). Expression levels of nsP3 and 14-3-3 ε prior to (left panel) and after (middle and right panels) GFP immunisolations were assessed by Western blot. The percentages loaded of the whole cell lysates or immunoprecipitates are indicated (bottom). To enable comparisons between the 3-h and all 10-h immunoprecipitated samples, the levels of each protein were analyzed on the same blot.

associates with nsP3 at early times but falls below our detection levels due to the low levels of the isolated complex. Despite these low levels, we were able to detect proteins (e.g. hnRNPs) that associated with nsP3 at early times. However, this result could be due to differences in the stoichiometry of these proteins with respect to nsP3. To determine whether the low levels of nsP3 were responsible for the failure to detect 14-3-3 at early times, we took two approaches to compensate for the different levels of nsP3: 1) performing immunisolations from fewer cells at a late (10 h) than an early (3 h) time point or 2) performing immunisolations from equal cell numbers from early and late time points but loading less of the late. For the first approach, we obtained samples from early and late times that contained equivalent amounts of nsP3 and immunisolated similar amounts of nsP3-GFP (Fig. 5, experiment #1). The total amount of 14-3-3 was higher in the 3-h lysate than the 10-h lysate due to the corresponding increased number of cells used to compensate for the nsP3 levels. However, 14-3-3 was not detected in the immunoisolation from the 3-h sample, while it was clearly present in the 10-h sample. For the second approach, we also obtained similar levels of nsP3 and confirmed the presence of 14-3-3 at 10 h of infection (Fig. 5, experiment #2). Together, the immunisolations (Fig. 2), co-localization (Fig. 3 and supplemental Fig. S13), and Western blot analyses prior to and following IP (Figs. 4 and 5) demonstrate that the 14-3-3-nsP3 interaction is temporally regulated.

Alphavirus Infections, but Not All RNA Virus Infections, Cause Redistribution of G3BP1—Similar to our observations with wild-type Sindbis, infection with Ross River, another *Alphavirus* genus member, generated the same G3BP1 redistribution (Fig. 6). This suggests that G3BP1 recruitment may be generally important during alphavirus infection. However, infection with the *Flavivirus* Yellow fever virus did not alter the G3BP1 subcellular localization (Fig. 6). Therefore, this redistribution is not a general feature of all positive strand RNA virus infections.

The Nuclear Transport Factor 2 (NTF2)-like Domain of G3BP1 Is Sufficient for Its Association with nsP3—G3BP1 was previously identified as binding to Ras-GTPase-activating protein (23) and has since been reported to have a variety of biological

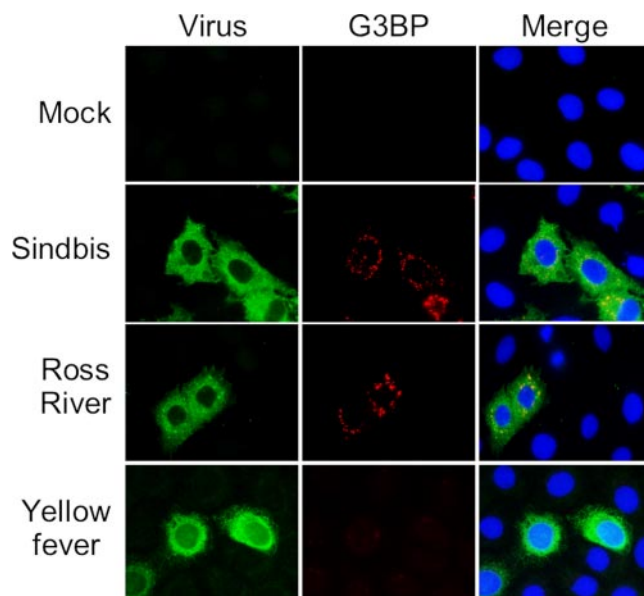


FIGURE 6. The G3BP1-nsP3 association is specific to alphaviruses. Rat2 cells were mock infected or infected (m.o.i. ~3) with the indicated wild-type viruses for 8 h (Sindbis, Ross River) or 20 h (Yellow fever) and were processed for fluorescence microscopy to detect G3BP1 (G3BP, red). Infected cells (Virus, green) were detected by staining for virus capsid protein (Sindbis, Ross River) or NS4 (Yellow fever). Nuclei (blue) are shown in the merged images.

activities (reviewed in Ref. 24). While the precise function of G3BP1 remains uncertain, conserved motifs have been noted (23, 25, 26), including an acidic domain, an RNA recognition motif (RRM), an RGG motif, and a NTF2-like domain (Fig. 7A). The motifs have been implicated in several interactions, for example the RRM and RGG motifs in RNA binding (27), the NTF2-like domain in G3BP1 protein multimerization, and the NTF2-like and RRM domains in stress granule localization (12). To map the interaction domain of G3BP1 with nsP3, we generated cells expressing GFP-tagged full-length G3BP1 or individual domains of G3BP1, previously described and termed A, B, C, and D (12). Western analysis demonstrated appropriate expression of the tagged proteins (supplemental Fig. S14). For co-localization studies of GFP-tagged G3BP1 proteins we generated a mutant Sindbis expressing nsP3 fused to the monomeric red fluorescent protein (mRFP-1 (10)). The mRFP tag was inserted in the same position as the GFP tag in the nsP3-GFP Sindbis mutant virus. Our results (Fig. 7B) showed co-localization of nsP3 with both the full-length G3BP1 and G3BP1 domain A, which exhibits homology to NTF2 (26). Co-localization with nsP3 was not observed for domains B, C, and D, although there was occasional overlap of staining for nsP3-mRFP and GFP-D.

Reciprocal immunisolations of G3BP1 were performed to verify the nsP3 interaction (Figs. 8 and 9). Cells expressing GFP-tagged G3BP1 (full-length ABCD) or the A–D domains were infected with wild-type Sindbis and used for immunisolations via the GFP tag. nsP3 interacted with both the NTF2 homology motif (A domain) and the full-length G3BP1 (ABCD), as determined by Western blot analysis (Fig. 8). No interaction was observed for domains B, C, or D. Mass spectrometry analyses of immunisolates from infected cells expressing GFP-tagged A domain and ABCD confirmed the presence of nsP3 in viral

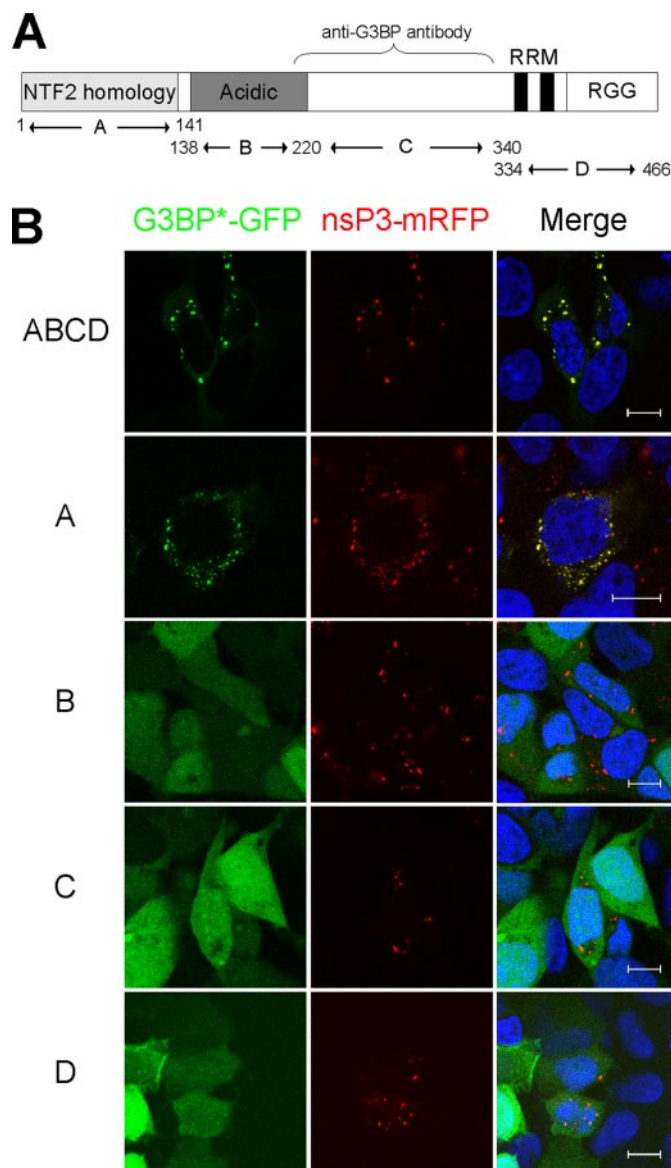


FIGURE 7. The G3BP1 NTF2-like domain is sufficient for association with nsP3. *A*, domains of G3BP1 protein: NTF2 homology, acidic domain, the RRM, and the RGG domain. The G3BP amino acids expressed as GFP fusion proteins in the expression constructs are indicated. *B*, confocal microscopy: HEK293 cells expressing GFP-tagged G3BP (ABCD) or GFP-tagged domains of G3BP (A, B, C, and D, as indicated) were infected with nsP3-mRFP-1 Sindbis (m.o.i. ~4). Cells were fixed for analysis by confocal microscopy after 14 h. The green (GFP-G3BP or GFP-G3BP domain, indicated as G3BP*-GFP), red (nsP3-mRFP), and merged images are shown. Nuclei (blue) are shown in the merged images. Bars, 5 μ m.

infected cells (Fig. 9). The A domain is known to mediate multimerization, and indeed endogenous G3BP was detected in immunisolations of GFP-A and GFP-ABCD from both uninfected and infected cells (Fig. 9). Together with the co-localization results, these findings indicate that the NTF2 homology domain of G3BP1 is necessary and sufficient for the observed G3BP-nsP3 interaction.

G3BP1 Interacts with Nuclear Pore Complex Proteins—In addition to providing a confirmation of the G3BP-nsP3 interaction and to mapping this interaction to the NTF2-like domain, the reciprocal immunisolations also identified novel G3BP-associated proteins. Members of the nuclear pore com-

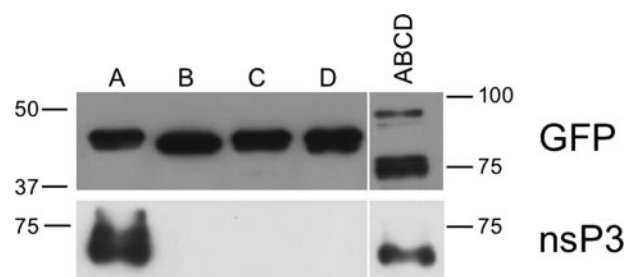
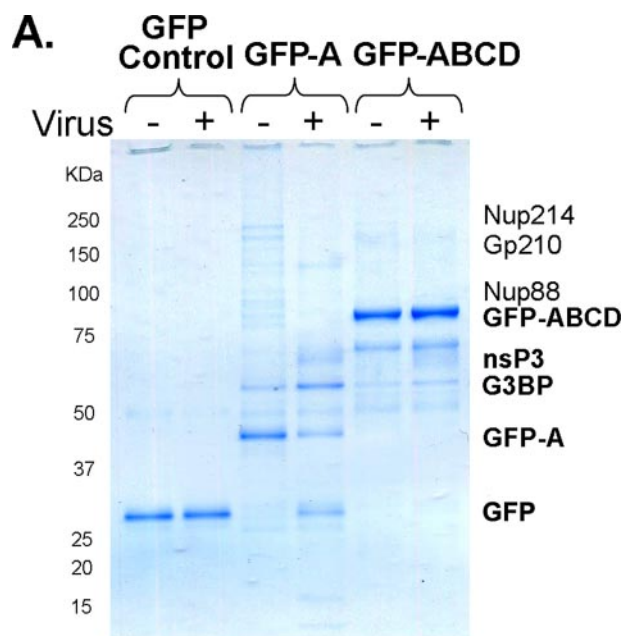


FIGURE 8. nsP3 associates with the NTF2-like domain and the full-length G3BP1. HEK293 cells stably expressing GFP-tagged versions of G3BP1 domains (A, B, C, D, and ABCD) were infected with wild-type Sindbis (m.o.i. ~15) for 15 h. A, B, C, D, and ABCD forms of G3BP1 were immunisolated via the GFP tag. Levels of isolated G3BP1 forms and nsP3 were assessed by Western blot as indicated.

plex, such as Nup214, gp210, and Nup88 (28, 29), were identified in G3BP isolates from uninfected and infected cells. Our isolations also confirmed the previously reported interaction of G3BP1 with ubiquitin specific protease 10 (USP10) (30). A G3BP-interacting protein isolated only from infected cells was 14-3-3. This protein was previously immunisolated and colocalized with nsP3-GFP (Figs. 2 and 3), indicating that 14-3-3 is likely to be present in this isolation due to its interaction with nsP3. The G3BP-associated proteins are summarized in Fig. 9 and supplemental Table S2.

nsP3 Partially Localizes to the Nuclear Envelope—We used electron microscopy to ascertain in greater detail the subcellular localizations of nsP3 in infected cells (Fig. 10). Morphological characteristics of infected Rat2 cells (Fig. 10, A and B) included cytoplasmic vacuoles with spherule invaginations, characteristic of alphavirus infection and likely sites of RNA replication and transcription (20, 31–33). In addition, aggregates of electron-dense granular material with irregular boundaries were specific to infected cells. These aggregates had the appearance of either rod-like (Fig. 10A) or round (Fig. 10B) electron-dense material, which might represent two types of aggregates or one structure observed from different planes of sectioning. Cytoplasmic electron-dense material, identified as containing Semliki Forest virus nsP3 by immunogold labeling, has been reported in both Semliki Forest virus-infected and nsP3-overexpressing HeLa cells (34). Using GFP immunogold labeling we detected Sindbis nsP3 in cytoplasmic aggregates (Fig. 10, C and D), likely corresponding to the electron-dense material seen in our morphological analyses (Fig. 10, A and B). In agreement with previous reports (20, 33), we also detected nsP3 on the cytoplasmic face of the cytoplasmic vacuoles and the plasma membrane (data not shown). In addition, we detected nsP3 at the nuclear envelope (Fig. 10E), which, considering the nsP3-G3BP association, may explain the reduced G3BP-nuclear pore interactions noticed upon infection (Fig. 9).

The Role of nsP3-associating Host Proteins during Infection—G3BP was detected as one of the main interacting partners of nsP3 at all studied times of infection. While the role of the G3BP recruitment in alphavirus replication is unclear, there is precedent for its involvement in viral replication, as G3BP1 has been found to be important for vaccinia virus intermediate stage transcription (35). G3BP has been implicated in a number of cellular processes, many of which suggest a possible role in



B.

	GFP-A		GFP-ABCD	
	Uninfected	Infected	Uninfected	Infected
Nup88	+++	+	++	+
Nup214	+++	+	++	+
gp210	+++	+	++	+
nsP3	-	+++	-	+++
14-3-3 ϵ	-	++	-	++
14-3-3 ζ	-	++	-	++
P120	+	+	+	+
Tpr	+	+	-	-
mrnp41	+	-	+	-
N-HSST	+	-	+	-
DOCK4	-	+	-	+
NT-AF3	-	-	+	-
USP10	-	-	++	++
KAB2	-	-	+	+
Shank2	-	-	-	+

FIGURE 9. Reciprocal immunoprecipitations indicate the association of G3BP1 with nuclear pore proteins. HEK293 cells stably expressing free GFP or GFP-tagged versions of G3BP1 domains were mock-infected (uninfected) or infected with wild type Sindbis (m.o.i. ~ 10) for 15 h. **A**, GFP-tagged A domain and ABCD domain were immunoprecipitated via the GFP tag from both uninfected (-) and infected (+) cells. Cells that express free GFP served as controls. Representative identified proteins are shown on the SDS-PAGE gel. Breakdown of GFP-A was observed in infected cells. **B**, relative levels of proteins identified in the immunoprecipitates of GFP-A and GFP-ABCD (uninfected and infected). Plus signs indicate the relative levels as assessed by semiquantitative mass spectrometry; minus signs indicate that the protein was not detected.

RNA metabolism or translation regulation (reviewed in Ref. 24). G3BP1 has been shown to assemble stress granules (12), sites of mRNAs coupled to abortive translation initiation complexes (reviewed in Ref. 36). Recent studies (37) on the related alphavirus Semliki Forest virus showed that stress granules are formed upon infection and correlate with host translational shutdown. Subsequent dissolution of the granules occurs at late times after infection and the infected cells lose their ability to assemble stress granules, as measured by T-cell intracellular antigen-1 (TIA-1) and eIF3 staining. The stress granules identified by TIA-1 staining after alphavirus infection are likely not the same structures as the cytoplasmic aggregates of nsP3 identified by us and others (34), since we did not identify TIA-1 in the nsP3 and G3BP containing complexes (supplemental Table S1) and TIA-1 did not co-localize with nsP3-GFP and G3BP (data not shown). However, since G3BP1 can assemble stress granules, the recruitment of this molecule into nsP3-containing complexes may influence TIA-1 containing stress granule formation (or dissolution). Alteration of the G3BP- or TIA-1-related stress granule pathway by the recruitment of G3BP by nsP3 might play a role in alphavirus control of cellular translation.

Our studies identified the NTF2-like domain of G3BP1 as the probable site of interaction with nsP3. The co-isolation of nuclear pore complex proteins with G3BP1, along with the RNA binding ability of G3BP, suggests that G3BP may function as a transport factor for RNA movement into or out of the nucleus, as suggested previously (38). Levels of G3BP-associated nuclear pore complex proteins were significantly reduced in infected cells, possibly due to the virus-induced subcellular redistribution of G3BP or to competition between nuclear pore proteins and nsP3 for binding to G3BP. Our finding that a subset of nsP3 localizes to the nuclear envelope suggests that, in addition to the cytoplasmic nsP3-G3BP association, an association between nsP3 and G3BP might also take place at the nuclear envelope. These results suggest that Sindbis may recruit G3BP as a means to block G3BP-dependent export (or import) of host mRNAs. Alternatively, host RNAs undergoing nuclear export may be captured for subsequent sequestration, resulting in translational shutoff. It is also possible that G3BP association with nsP3 represents a specific host response to counteract alphavirus infection.

Several hnRNP proteins (A1, A2/B1, G, and A3) were also identified in the nsP3-GFP-containing complexes. Members of the hnRNP family have been found to be involved in other virus life cycles, including activation of poxvirus late transcription (39) and in the regulation of mouse hepatitis virus RNA replication (40–42). These RNA-binding proteins might be specifically recruited or could be present due to their presence on RNA molecules, bound, for example, to G3BP. Decreased amounts of hnRNP proteins in the nsP3-containing complexes at the later infection time points could be due to decreased expression levels, degradation, or altered binding to the complexes.

Another isolated interacting partner of nsP3, 14-3-3, may also reflect viral control of important cellular processes. 14-3-3, a phosphoserine-binding adapter protein involved in

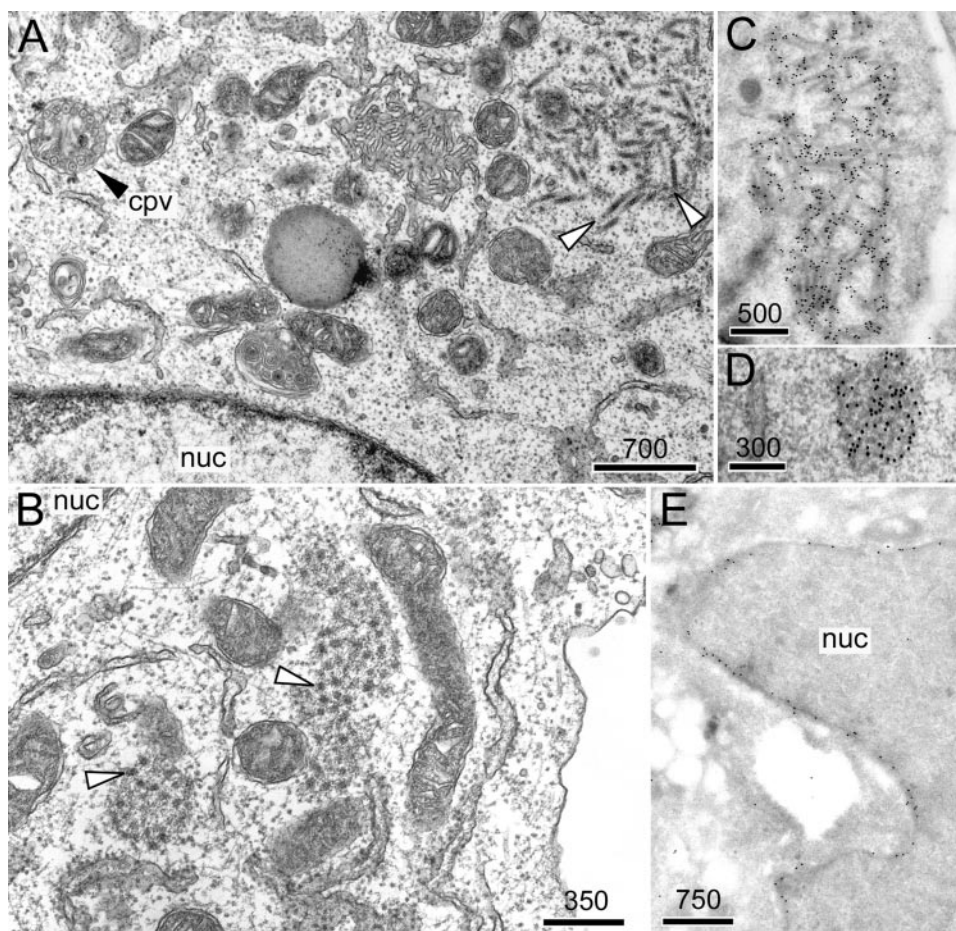


FIGURE 10. Immunogold EM localizes nsP3-GFP to multiple sites in infected cells. A and B, morphological evaluation of infected Rat2 cells. Cytopathic vacuoles (cpv) with spherules (A, dark arrowhead) as well as aggregates of electron-dense rod-like (A) and round (B) structures (white arrowheads) were specific to infected cells. C–E, immunogold (10 nm) labeling of cryosections from infected cells using anti-GFP antibodies localizes nsP3-GFP to cytoplasmic aggregates of rod-like (C) and round (D) material. Labeling of the nuclear membrane (E) was also observed. nuc, nucleus; bars, distances in nm.

CONCLUSIONS

These studies utilized natural viral infection with differentially tagged GFP-expressing alphaviruses and high titer anti-GFP antibodies for the efficient isolation of protein complexes. We determined the viral and host proteins that interact with Sindbis nsP3 during the course of infection of vertebrate cells. These results led to several interesting hypotheses regarding the manipulation of cellular processes by Sindbis. It should be possible to build a comprehensive picture of the complex alphavirus-host relationship using mutant viruses that express GFP on alternative viral proteins or are mutated or deficient in specific viral proteins. Animal models can be studied using a similar approach to investigate virus replication, spread, and pathogenesis *in vivo*. These techniques depend on the ability to insert a tag within a protein without disrupting viral function. Although this will not always prove feasible, several viable GFP-tagged viruses have already been utilized for visualization studies. Therefore, we predict that the presently described techniques, which should be broadly applicable to many viral systems, will greatly facilitate our understanding of the molecular details of viral infections and the biology of the cell.

regulating cell signaling pathways (reviewed in Ref. 43), was observed to associate with nsP3 in a time-dependent manner. Experiments utilizing equivalent amounts of nsP3 from early and late stages of infection verified that the nsP3–14-3-3 association occurs only at late times. This implies a change in the state of the interacting partner of 14-3-3, which could be a phosphorylation event. Two likely candidates are nsP3 itself and G3BP, both known to be phosphorylated on serine residues (44, 45). The recruitment of 14-3-3 might be important for host translational shutoff, the shutoff of minus strand synthesis, or other processes that are time-dependent in infected cells. Interestingly, Sindbis infection is known to activate stress responses including the p38 mitogen-activated protein kinase signaling cascade (46), implicated in the posttranscriptional regulation of gene expression (reviewed in Ref. 47). Phosphorylation of tristetraprolin (TTP) induced by this pathway has been suggested to result in 14-3-3 binding to TTP, which blocks TTP movement to stress granules and inhibits TTP-mediated mRNA decay (48). 14-3-3 recruitment to nsP3-containing complexes may alter mRNA trafficking or decay or affect other signaling pathways.

Acknowledgments—We are grateful to Dr. Guangpu Li for providing *pToto1101/GFP*. We thank Dr. Jamal Tazi for GFP-tagged *G3BP1* expression plasmids, Dr. Roger Tsien for *mRFP-1* encoding DNA, Dr. Alison North for advice regarding confocal microscopy, and Helen Shio for electron microscopy work. We thank Joe Marcotrigiano for critical help in initiating this project.

REFERENCES

- Cristea, I. M., Williams, R., Chait, B. T., and Rout, M. P. (2005) *Mol. Cell. Proteomics* **4**, 1933–1941
- Griffin, D. E. (2001) in *Fields Virology* (Knipe, D. M., and Howley, P. M., eds) Fourth Ed., pp. 917–962, Lippincott Williams & Wilkins, Philadelphia
- Schlesinger, S., and Schlesinger, M. J. (2001) in *Fields Virology* (Knipe, D. M., and Howley, P. M., eds) Fourth Ed., pp. 895–916, Lippincott Williams & Wilkins, Philadelphia
- Strauss, J. H., and Strauss, E. G. (1994) *Microbiol. Rev.* **58**, 491–562
- Kääriäinen, L., and Ahola, T. (2002) *Prog. Nucleic Acids Res. Mol. Biol.* **71**, 187–222
- Liang, Z., and Li, G. (2005) *Gene Ther. Mol. Biol.* **9**, 317–324
- Lastarza, M. W., Grakoui, A., and Rice, C. M. (1994) *Virology* **202**, 224–232
- Bick, M. J., Carroll, J.-W. N., Gao, G., Goff, S. P., Rice, C. M., and

- MacDonald, M. R. (2003) *J. Virol.* **77**, 11555–11562
9. Rice, C. M., Levis, R., Strauss, J. H., and Huang, H. V. (1987) *J. Virol.* **61**, 3809–3819
 10. Campbell, R. E., Tour, O., Palmer, A. E., Steinbach, P. A., Baird, G. S., Zacharias, D. A., and Tsien, R. Y. (2002) *Proc. Natl. Acad. Sci. U. S. A.* **99**, 7877–7882
 11. Frolova, E. I., Fayzulin, R. Z., Cook, S. H., Griffin, D. E., Rice, C. M., and Frolov, I. (2002) *J. Virol.* **76**, 11254–11264
 12. Tourriere, H., Chebli, K., Zekri, L., Courselaud, B., Blanchard, J. M., Bertrand, E., and Tazi, J. (2003) *J. Cell Biol.* **160**, 823–831
 13. Rice, C. M., and Strauss, J. H. (1982) *J. Mol. Biol.* **154**, 325–348
 14. Chambers, T. J., McCourt, D. W., and Rice, C. M. (1989) *Virology* **169**, 100–109
 15. Harlow, E., and Lane, D. (1988) in *Antibodies, A Laboratory Manual*, pp. 312–318, Cold Spring Harbor Laboratory, Cold Spring Harbor, NY
 16. Barton, D. J., Sawicki, S. G., and Sawicki, D. L. (1991) *J. Virol.* **65**, 1496–1506
 17. Cristea, I. M., Gaskell, S. J., and Whetton, A. D. (2004) *Blood* **103**, 3624–3634
 18. Tokuyasu, K. T. (1986) *J. Microsc. (Oxf.)* **143**, 139–149
 19. Griffiths, G., Simons, K., Warren, G., and Tokuyasu, K. T. (1983) *Methods Enzymol.* **96**, 466–485
 20. Froshauer, S., Kartenbeck, J., and Helenius, A. (1988) *J. Cell Biol.* **107**, 2075–2086
 21. Frolova, E., Gorchakov, R., Garmashova, N., Atasheva, S., Vergara, L. A., and Frolov, I. (2006) *J. Virol.* **80**, 4122–4134
 22. Archambault, V., Chang, E. J., Drapkin, B. J., Cross, F. R., Chait, B. T., and Rout, M. P. (2004) *Mol. Cell* **14**, 699–711
 23. Parker, F., Maurier, F., Delumeau, I., Duchesne, M., Faucher, D., Debussche, L., Dugue, A., Schweighoffer, F., and Tocque, B. (1996) *Mol. Cell. Biol.* **16**, 2561–2569
 24. Irvine, K., Stirling, R., Hume, D., and Kennedy, D. (2004) *Int. J. Dev. Biol.* **48**, 1065–1077
 25. Kennedy, D., Wood, S. A., Ramsdale, T., Tam, P. P., Steiner, K. A., and Mattick, J. S. (1997) *Biomed. Pept. Proteins Nucleic Acids* **2**, 93–99
 26. Suyama, M., Doerks, T., Braun, I. C., Sattler, M., Izaurralde, E., and Bork, P. (2000) *EMBO Rep.* **1**, 53–58
 27. Tourriere, H., Gallouzi, I. E., Chebli, K., Capony, J. P., Mouaikel, J., van der Geer, P., and Tazi, J. (2001) *Mol. Cell. Biol.* **21**, 7747–7760
 28. Cronshaw, J. M., Krutchinsky, A. N., Zhang, W., Chait, B. T., and Matunis, M. J. (2002) *J. Cell Biol.* **158**, 915–927
 29. Suntharalingam, M., and Wenthe, S. R. (2003) *Dev. Cell* **4**, 775–789
 30. Soncini, C., Berdo, I., and Draetta, G. (2001) *Oncogene* **20**, 3869–3879
 31. Grimley, P. M., Berezesky, I. K., and Friedman, R. M. (1968) *J. Virol.* **2**, 1326–1338
 32. Peranen, J., and Kääriäinen, L. (1991) *J. Virol.* **65**, 1623–1627
 33. Kujala, P., Ikaheimonen, A., Ehsani, N., Vihinen, H., Auvinen, P., and Kääriäinen, L. (2001) *J. Virol.* **75**, 3873–3884
 34. Salonen, A., Vasiljeva, L., Merits, A., Magden, J., Jokitalo, E., and Kääriäinen, L. (2003) *J. Virol.* **77**, 1691–1702
 35. Katsafanas, G. C., and Moss, B. (2004) *J. Biol. Chem.* **279**, 52210–52217
 36. Anderson, P., and Kedersha, N. (2002) *J. Cell Sci.* **115**, 3227–3234
 37. McInerney, G. M., Kedersha, N. L., Kaufman, R. J., Anderson, P., and Liljestrom, P. (2005) *Mol. Biol. Cell* **16**, 3753–3763
 38. Prigent, M., Barlat, I., Langen, H., and Dargemont, C. (2000) *J. Biol. Chem.* **275**, 36441–36449
 39. Wright, C. F., Oswald, B. W., and Dellis, S. (2001) *J. Biol. Chem.* **276**, 40680–40686
 40. Choi, K. S., Mizutani, A., and Lai, M. M. (2004) *J. Virol.* **78**, 13153–13162
 41. Shi, S. T., Huang, P., Li, H. P., and Lai, M. M. (2000) *EMBO J.* **19**, 4701–4711
 42. Shi, S. T., Yu, G. Y., and Lai, M. M. (2003) *J. Virol.* **77**, 10584–10593
 43. Mackintosh, C. (2004) *Biochem. J.* **381**, 329–342
 44. Li, G. P., La Starza, M. W., Hardy, W. R., Strauss, J. H., and Rice, C. M. (1990) *Virology* **179**, 416–427
 45. Gallouzi, I. E., Parker, F., Chebli, K., Maurier, F., Labourier, E., Barlat, I., Capony, J. P., Tocque, B., and Tazi, J. (1998) *Mol. Cell. Biol.* **18**, 3956–3965
 46. Nakatsue, T., Katoh, I., Nakamura, S., Takahashi, Y., Ikawa, Y., and Yoshinaka, Y. (1998) *Biochem. Biophys. Res. Commun.* **253**, 59–64
 47. Clark, A. R., Dean, J. L., and Saklatvala, J. (2003) *FEBS Lett.* **546**, 37–44
 48. Stoecklin, G., Stubbs, T., Kedersha, N., Wax, S., Rigby, W. F., Blackwell, T. K., and Anderson, P. (2004) *EMBO J.* **23**, 1313–1324